Environmental Science & Technology

pubs.acs.org/est

Article

Observations of Nocturnal Sulfuric Acid Formation in Pittsburgh, PA

Dominic A. Casalnuovo, Darren Cheng, Christine Troller, Ziheng Zeng, Albert A. Presto, and Coty N. Jen*

Cite This: https://doi.org/10.1021/acs.est.5c14137

Read Online

ACCESS | Metrics & More | Article Recommendations | Supporting Information

ABSTRACT: Measurements of sulfuric acid (H_2SO_4) and sulfur trioxide (SO_3) were conducted in Pittsburgh, Pennsylvania, during field campaigns in Fall 2023 and Fall 2024. These measurements identified nocturnal concentrations of H_2SO_4 comparable to those of daytime values. Nocturnal H_2SO_4 concentrations were observed to increase by 5×10^5 to 5×10^7 molecules cm^{-3} above background on 16 of the 31 measurement nights. The median peak concentration during events was 6.5×10^6 molecules cm^{-3}, with a maximum of 1.0×10^8 molecules cm^{-3}, exceeding previously reported nighttime concentrations. Increases in H_2SO_4 concentrations were positively correlated with the anomalously high SO_3 concentrations and condensation sink rates, indicating that the formation of H_2SO_4 increased to overcome the loss rates to particles. Increases in particulate mass and the mass fraction of metals commonly emitted from coal combustion and steel production were also observed. The air masses were traced back to the southeast of Pittsburgh, a region home to a steel mill, coke plant, and a steel processing plant. The observations indicate a previously unrecognized nighttime formation pathway for H_2SO_4, potentially from heterogeneous catalysis with metal or black carbon, originating from steel and coke plant emissions. Further measurements are needed to identify key compounds and chemical processes driving these increases in nocturnal H_2SO_4 concentrations.

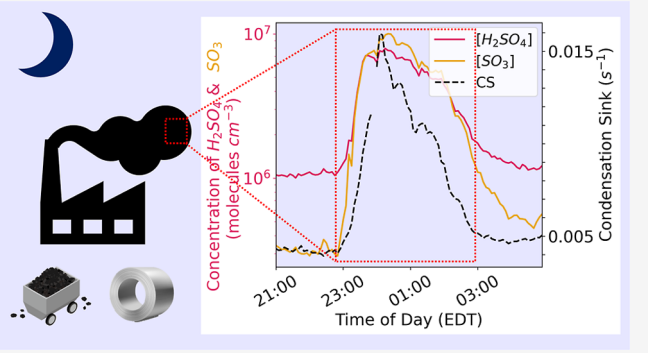

KEYWORDS: *sulfuric acid, sulfur trioxide, nocturnal chemistry, aerosols, steel emissions, coal burning, oxidation, particulate metals*

1. INTRODUCTION

Atmospheric sulfuric acid vapor plays an important role in the Earth's radiative balance through new particle formation (NPF) and particle growth.[1−5] NPF consists of the formation of stable particles via the reactions of gases and the subsequent growth of these particles to larger sizes. NPF processes produce roughly 50% of the global number of cloud condensation nuclei (CCN) and thus affect cloud formation and properties.[1−3,6] Previous field observations have shown that atmospheric sulfuric acid vapor (H_2SO_4) is the key compound for NPF in most regions of the world.[7−9] H_2SO_4 vapor also changes atmospheric particle composition and size through its condensation onto aerosol particles.[4,5] However, uncertainty in modeling H_2SO_4 concentrations affects the predicted atmospheric aerosol concentration and composition.[1,2]

One contributing factor to the uncertainty in H_2SO_4 concentrations is the difficulty in modeling its formation pathways and rate of accumulation in the atmosphere.[10,11] During the day, the formation pathway for H_2SO_4 is driven by photochemistry. Sulfur dioxide (SO_2) is oxidized by hydroxyl radicals (OH), which are formed through the photodissociation of ozone (O_3), nitrous acid (HONO), and formaldehyde (HCHO).[10,12−15] As OH oxidizes SO_2 to form sulfur trioxide (SO_3), SO_3 is rapidly converted to H_2SO_4 in less than a second via reactions with water[16] and catalyzed by acids and ammonia.[17−19] Daytime concentrations of H_2SO_4 span many orders of magnitude, with observations ranging from $\sim 1 \times 10^5$ to 3×10^8 molecules cm^{-3}, while nocturnal concentrations are usually 10^6 molecules cm^{-3} or below.[7,12,20] However, recent field campaigns in Beijing, China, and Hyytiälä Forest, Finland, indicate that nonphotochemical sources can contribute to the formation of SO_3 and H_2SO_4 at night and during the early morning.[12,20,21] In Hyytiälä Forest during 2010, the maximum nighttime concentration of H_2SO_4 reached $\sim 1 \times 10^7$ molecules cm^{-3}.[20] Despite the high nocturnal concentrations of H_2SO_4 observed in Hyytiälä, concentrations of H_2SO_4 generally decreased at night, with the highest nocturnal concentration observed at sunset. In Beijing, nocturnal increases in H_2SO_4 were attributed to its formation from stabilized Criegee intermediates (SCI) and a decrease in the condensation sink (CS), the loss rate of H_2SO_4 to preexisting particles.[12] Criegee

Received: October 7, 2025
Revised: March 31, 2026
Accepted: March 31, 2026

intermediates form when O_3 reacts with alkenes.[12,20,22] In the atmosphere, roughly half of the Criegee intermediates break down to form OH in less than a second[22] with a small fraction forming dioxiranes and secondary ozonides.[23,24] The other half is stabilized and forms SCI, which is capable of oxidizing SO_2 directly into SO_3 and ultimately H_2SO_4. Due to the short lifetime of H_2SO_4 in the atmosphere (~1 min in a polluted urban environment), this compound was likely formed via nocturnal oxidation of SO_2 and not from long-range transport.[12,21]

Catalytic oxidation of SO_2 at the surface of traffic-related particles containing black carbon (BC) was also suggested to occur in Beijing during the early mornings when OH concentrations were low.[21] In the winter, increasing SO_3 concentration was observed in the early morning, suggesting that the formation pathway was not photochemically driven. These field measurements are supported by laboratory and computational studies that showed carbon-containing aerosols oxidizing SO_2.[25] The measurements from Beijing revealed that the formation of SO_3 and H_2SO_4 correlated with the increased concentration of sub-2.5 nm particles in the early morning. As a result, aerosols containing BC induced the formation of H_2SO_4 and could ultimately influence the daytime particle concentration.[21]

This study presents nighttime observations of H_2SO_4 from Pittsburgh, PA located in Allegheny County. The nocturnal trends of H_2SO_4 exhibit distinctly different patterns from those observed in previous studies.[12,20,21] Pittsburgh experiences a wide mixture of emissions typical of an urban environment with additional major contributions from the Mon Valley Works (MVW) complex. The MVW complex consists of a steel mill (Edgar Thompson Plant), a coke plant (Clairton Plant), and a steel processing plant (Irvin Plant), which are located 10−15 km to the southeast of Pittsburgh. The MVW complex has previously been reported to be a large source of SO_2 and hydrogen sulfide (H_2S).[26−28] Specifically, the 2022 Allegheny County emission database showed that the Clairton Plant had the highest reported annual emissions of SO_2, H_2S, and particulate matter smaller than 2.5 μm in diameter ($PM_{2.5}$) in Allegheny County.[27,28] The Edgar Thompson Plant and Irvin Plant had the second and fourth highest sulfur oxides and $PM_{2.5}$ emissions, respectively.[27] In addition to sulfur compounds and $PM_{2.5}$, extended measurements near the MVW complex and previous studies have shown coal burning can emit high concentrations of BC and trace metals, such as selenium, zinc, manganese, and iron.[29−33]

To better understand the sources of nocturnal H_2SO_4 in Pittsburgh, we measured atmospheric gas concentrations, particle size distributions, and particle composition. During the campaign, we consistently observed events where the concentrations of H_2SO_4 and SO_3 increased during the night, with the median peak concentrations of 6.5×10^6 and 9.0×10^6 molecules cm^{-3}, respectively, when resampled with a 5 min average. The maximum observed nighttime concentrations of H_2SO_4 and SO_3 were 1.0×10^8 and 1.6×10^8 molecules cm^{-3}, respectively, which are larger than any nighttime observations in Beijing or Hyytiälä.[12,20,21] The nighttime measurements of H_2SO_4 during events were the same order of magnitude as daytime concentrations, which are known to impact the climate.[1,5,7] Using measurements of trace atmospheric gases, particle composition, and meteorological conditions, we investigated the potential sources of air containing the increased H_2SO_4 concentrations and drivers of these events.

2. MATERIALS AND METHODS

2.1. Carnegie Mellon University Sampling Site

The main measurement site was located on the Carnegie Mellon University (CMU) campus in Doherty Hall (see Figure S1 in the Supporting Information, SI). Two measurement campaigns were conducted: September 21st, 2023 to October 14th, 2023 and October 4th, 2024 to October 16th, 2024. The nighttime temperature ranged from 8 to 33 °C (mean of 17 ± 4.7 °C) with a relative humidity from 27 to 92% (mean of 64% ± 15%). During the 2023 campaign, instruments sampled from the third floor of the south side of the building, which overlooks a grassy quadrangle and a large park. In contrast, the instruments sampled from the first floor of Doherty Hall from a north-facing window during the 2024 campaign, see Figure S2. The north side of the building is more sheltered, with sections of the building to the east and west that extend past the window. The north side overlooks the building's exhaust vents. Since the building is built on a hill, both the third-floor and the first-floor sample locations are ~15 m above ground level.

H_2SO_4 and SO_3 were measured by an atmospheric pressure interface long time-of-flight chemical ionization mass spectrometer (CIMS) with a custom-built transverse inlet using nitrate reagent ions (NO_3^-, $HNO_3{\cdot}NO_3^-$, and $H_2O{\cdot}NO_3^-$).[34−38] Dominant signals for H_2SO_4 were HSO_4^- and $HNO_3{\cdot}HSO_4^-$. For SO_3, the observed signals included SO_4^- and $SO_3{\cdot}NO_3^-$. Only the $SO_3{\cdot}NO_3^-$ signal was included in the conversion to concentration as SO_4^- can also be formed from SO_2 within the chemical ionization inlet.[21] Signals were converted to concentrations following ionization kinetics and are detailed in the Supporting Information.[35,39] The CIMS sampled at 15 LPM through an ~100 cm long, 5 cm ID glass sample tube extending ~50 cm outside the window. The chemical ionization reaction times were 0.018 and 0.016 s for the 2023 and 2024 campaigns, respectively. The selected chemical ionization reaction times allowed for the ionization of species such as H_2SO_4 and SO_3 while limiting the products of chemical ionization reactions (and other ions produced by the radioactive source) from subsequent ionization of other atmospheric molecules. Ionization rate coefficients of 1.9×10^{-9} cm^3 s^{-1} and 9.3×10^{-10} cm^3 s^{-1} were used for H_2SO_4 and SO_3 ionized by nitrate ions, respectively.[40,41] In addition, CIMS signals were corrected for mass-dependent transmission efficiency measured on a similar instrument and diffusional wall loss for a similar glass sampling tube.[42−44] The CIMS inlet and sampling flow were previously examined in the laboratory to ensure <30 s response time to a factor of 10−100 decrease in the H_2SO_4 concentration. Thus, the observations reported in this study reflect the changing sulfuric acid concentration within a 1 min time scale. See the Supporting Information for more discussion on the CIMS signal to concentration conversion.

During the campaigns, the 1.6−300 nm particle size distribution was measured by two stepping mobility particle sizing devices known as the particle sizing devices (PSD). The CS was calculated from the particle size distribution.[45−48] The PSD sampled from a 10 cm ID community inlet, which operated at >250 LPM flow. The community inlet extended 1 m from the window and faced the same direction as the CIMS sample tube. More details on sampling for the PSD are provided in Cheng et al.[49] Mass concentration of particulate matter smaller than 2.5 μm in diameter ($PM_{2.5}$) was measured by a PurpleAir Flex sensor, located 250 m northeast of Doherty Hall, see Figure S2.

2.2. Supporting Observations at Lawrenceville, North Braddock, and Liberty

Additional gas and particle phase measurements were conducted by the Allegheny County Health Department (ACHD) and the Atmospheric Science and Chemistry mEasurement NeTwork (ASCENT) as part of permanent measurement sites in Pittsburgh.[50,51] A map of all measurement sites is given in Figure S1. ACHD and ASCENT are located 3 km northwest of the CMU measurement site in Lawrenceville, PA. These measurements included SO_2 (Teledyne API (TAPI) 100 EU), O_3 (Thermo 49), NO_2 (TAPI N500), NO_y (TAPI 200 EU), $PM_{2.5}$ (Thermo RP Partisol-Plus 2025),

https://doi.org/10.1021/acs.est.5c14137
Environ. Sci. Technol. XXXX, XXX, XXX−XXX

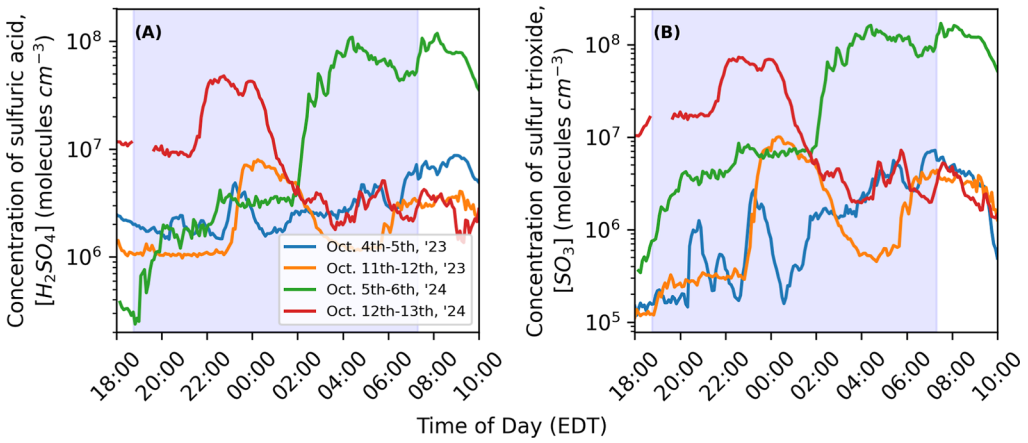

Figure 1. Example events where concentrations of (A) H_2SO_4 and (B) SO_3 increased during the night in Pittsburgh, PA. Each color represents a different date, with shaded regions indicating the hours between sunset and sunrise.

BC (TAPI 633), and particulate metal concentration (Xact 625i). Ultraviolet radiation was measured with a Met One 094−1/6676. A Vaisala CL−51 ceilometer was used to determine the boundary layer height. The optimized Emeis method was used to calculate boundary layer height from the backscattering profiles.[52,53] Additional gas monitors managed by ACHD were located in North Braddock, PA, and Liberty, PA, which are 10 and 15 km to the southeast of CMU, respectively. The North Braddock and Liberty monitors are near the MVW complex.

The ASCENT Site also included a 3839W89 scanning mobility particle sizer to measure the particle size distribution from 10 to 800 nm. This instrument was not operational during these campaigns, but its long-term observations showed particle concentrations above 300 nm of <10 particles cm^{-3}. As a result, the CS determined from the PSD-measured 1.6−300 nm size distribution is representative of Pittsburgh air during the campaigns.

2.3. Plume Models and Citizen Science Measurements

Community-based observations were used to track the movement of polluted air masses and identify sulfur odors. Smell Pittsburgh (SmellPGH) is a mobile application where users report poor air quality, including the perceived severity, location, and an optional description of the smell.[54] Reports were filtered to include only those within the Pittsburgh city limits, shown in Figure S1.

$PM_{2.5}$ measured by ACHD and publicly available PurpleAir sensors were used to track the movement of plumes containing particles.[55] The $PM_{2.5}$ measurements were interpreted alongside Plume Pittsburgh, which uses the National Oceanic and Atmospheric Administration's High-Resolution Rapid Refresh (HRRR) model to simulate plume transport from the MVW complex plants located southeast of the city.[56]

3. RESULTS AND DISCUSSION

The CIMS measured frequent increases in the concentrations of nocturnal H_2SO_4 and SO_3 during the 2023 and 2024 campaigns. Figure 1 shows examples of H_2SO_4 and SO_3 concentration timelines for four nights with these nocturnal H_2SO_4 events. An event was defined by an increase in the H_2SO_4 concentration of more than 5×10^5 molecules cm^{-3} or SO_3 concentration of more than 3×10^5 molecules cm^{-3} over any 30 min period between sunset and sunrise. This threshold was empirically chosen based on the distribution of increases in H_2SO_4 and SO_3 across both campaigns. Examples of nonevent nights are shown in Figure S3. Over the course of 31 days of both campaigns, a total of 16 events were observed. Of the two campaigns, 2024 had a higher number of events, with an event occurring on all 12 nights. Sample event nights are shown in Figure 1 and exhibit an increase in H_2SO_4 and SO_3 concentrations at all times of the night. For example, the event on October 5th, 2024 started shortly after sunset, whereas the events on October 5th, 2023 and October 6th, 2024 began around midnight and persisted past sunrise. The nighttime concentrations of H_2SO_4 and SO_3 ranged from below detection limits of $\sim 2 \times 10^5$ and $\sim 1 \times 10^5$ molecules cm^{-3}, respectively, to 1.0×10^8 and 1.6×10^8 molecules cm^{-3}, respectively. Nocturnal H_2SO_4 concentrations during events were comparable to daytime values, which were generally on the order of 10^6 to 10^7 molecules cm^{-3}. In addition to high peak concentrations, nocturnal events could persist for hours, with multiple events occurring on some nights, such as on October 11th−12th, 2023, which had events at 23:00 and 06:00 EDT.

Nocturnal background concentrations of H_2SO_4 were high at $\sim 2 \times 10^6$ molecules cm^{-3} on most event and nonevent nights (Figure 1A), higher than those observed in Beijing (1×10^6 molecules cm^{-3}).[12,21] Furthermore, background concentrations of SO_3 were lower than H_2SO_4 in the Fall of 2023, often $\sim 2 \times 10^5$ molecules cm^{-3} during both event and nonevent nights. During the Fall of 2024 event nights, background concentration of SO_3 ranged from $\sim 2 \times 10^5$ to 4×10^6 molecules cm^{-3}, which was higher than background H_2SO_4, which ranged from $\sim 1 \times 10^5$ to 2×10^6 molecules cm^{-3}. Background concentrations of SO_3 were higher in Pittsburgh than in Beijing, which had a median background concentration of 3×10^5 molecules cm^{-3} during the winter.[21]

Although the background concentrations of H_2SO_4 and SO_3 varied depending on the night, the changes in the concentration were strongly correlated. The Spearman correlation coefficient of SO_3 with H_2SO_4 for each night across both campaigns is shown in Figure S4, where 14 out of the 16 event nights exhibited correlation coefficients greater than 0.9. The consistent correlation indicates that the formation of H_2SO_4 is driven by the hydrolysis of SO_3, which aligns with previous observations of nighttime H_2SO_4.[12,20,21] The observed high concentrations of SO_3 on event nights also imply that SO_3 and H_2SO_4 are being formed near the CMU measurement site, as SO_3 is converted to H_2SO_4 in the atmosphere in less than 1 s and cannot be transported long distances.[16,21]

The ratio of SO_3 to H_2SO_4 during these nighttime events ranged from 0.2 to ~2 similar to those observed during polluted nights in Beijing.[12,21] This ratio is dramatically higher

https://doi.org/10.1021/acs.est.5c14137
Environ. Sci. Technol. XXXX, XXX, XXX−XXX

than what was observed during the daytime, which ranged from ~0.3 to below the detection limit (see Figure S5), and nights without events (~0.2, see Figure S3). However, unlike Beijing with maximum SO_3 concentrations of 1.7×10^6 molecules cm^{-3}, the Pittsburgh SO_3 concentrations reached up to 10^8 molecules cm^{-3}. SO_3 rapidly reacts with water which implies that the high SO_3 concentration will result in an extremely fast production rate of H_2SO_4.[16] For example, on October 12th, 2024 (Figure 1), the peak SO_3 concentration was approximately 7×10^7 molecules cm^{-3} with a temperature of 15.5 °C and a dew point of 5 °C. This translates to a H_2SO_4 production of ~10^{12} molecules cm^{-3} s^{-1} (see Lovejoy et al.).[16] This production rate far exceeds the observed H_2SO_4 concentration of 4×10^7 molecules cm^{-3} even when taking into account a H_2SO_4 loss to pre-existing particles of ~0.01 s^{-1}. In contrast, the SO_3 concentration observed during the day was much lower, typically below the detection limit of ~1×10^5 molecules cm^{-3}. As a result, the anomalously high observed SO_3 concentration must also reflect unknown chemistry either in the atmosphere or in the nitrate CIMS inlet, which would only enhance the signal at $SO_3 \cdot NO_3^-$ measured by the CIMS at night.

Regardless of the accuracy of SO_3 concentrations, the clear trends in increasing H_2SO_4 and SO_3 signals during the event nights could be the result of several phenomena. One phenomenon is the contracting atmospheric boundary layer, which reduces the volume in the boundary layer and increases the concentration and coagulation of particles. The boundary layer typically collapses shortly after sunset. For example, on October 11th, 2023 as shown in Figure 2, the boundary layer height was ~400 m before sunset and rapidly reduced to ~80 m between 19:00 and 20:00 EDT. This effect can be seen in the particle size distribution shown in Figure 2A between 18:30 and 19:30 EDT on October 11th, 2023. The total concentration of particles rapidly increased with the mode diameter shifting from 15 nm at 18:30 to 26 nm at 19:30 EDT.

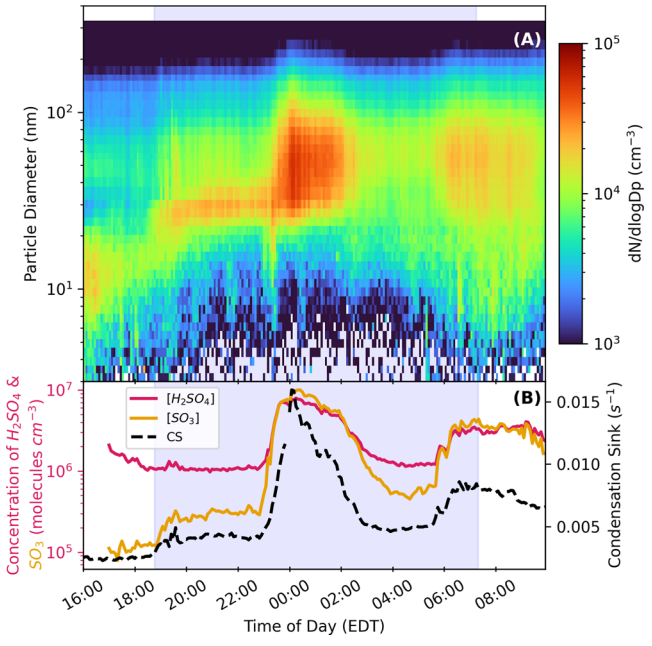

Figure 2. (A) Particle size distribution and (B) H_2SO_4 and SO_3 concentration, and condensation sink (CS) for October 11th–12th, 2023.

However, the H_2SO_4 events depicted in Figure 2B occur more than two hours after the boundary layer collapsed. As a result, the changing boundary layer is not the cause of these H_2SO_4 and SO_3 events.

The increase in H_2SO_4 at night could also be explained by a decrease in CS, the loss rate of H_2SO_4 to preexisting particles, combined with a constant formation rate of H_2SO_4 by SCI. In Beijing, the H_2SO_4 events had a negative correlation with CS. Figure 2 demonstrates that concentrations of 20–200 nm aerosol particles and their mode diameter (from 30 to 50 nm) increased with increasing H_2SO_4 as seen in Figure 2 at 23:00. The increase in size and concentration translates to a higher CS,[12,45,46] which correlates well with H_2SO_4 and SO_3 concentrations (see Figure S4) but anticorrelates during the day (Figure S5). The high CS at night likely explains why the increase in H_2SO_4 did not result in the formation of new particles (Figures 2 with more discussion in the Supporting Information). In contrast to the observations from Beijing, the positive correlations of H_2SO_4 with CS at night in Pittsburgh imply that the formation rate of H_2SO_4 must increase to compensate for the increased loss rate. Furthermore, H_2SO_4 and SO_3 must be formed near the sampling site, as both compounds have short lifetimes (less than 100 and 1 s, respectively) due to the high CS loss rate.[21,46–48]

One way the formation rate increases is if the concentration of SCI increased during the events. From Guo et al., the formation rate of H_2SO_4 from SCI can be approximated as $k_{app}[SO_2][O_3][\text{Alkenes}]$, where k_{app} is an empirically fitted rate coefficient ranging from 1.5×10^{-30} to 2.7×10^{-30} cm^6 s^{-1}.[12] The concentrations of alkenes were not measured during the Pittsburgh campaigns. To estimate the required alkene concentration to form the H_2SO_4 concentrations observed during the events, the steady-state H_2SO_4 chemical balance from Guo et al. can be solved for the alkene concentration (eq 1), where β is the hard-sphere collision rate between H_2SO_4 molecules with a value of 3.47×10^{-10} cm^3 s^{-1}.[12]

$$[\text{Alkenes}] = \frac{(\text{CS}[H_2SO_4] + \beta[H_2SO_4]^2)}{k_{app}[SO_2][O_3]} \quad (1)$$

On October 11th and 12th, 2023 (Figure 2) from 22:00 to 4:00, the $[SO_3]$ and $[O_3]$ were measured at a maximum of 0.6 and 1 ppb, respectively, in Lawrenceville. As such, the calculated concentration of alkenes needed to explain the rise in the observed H_2SO_4 concentrations is 1×10^{11} molecules cm^{-3} at 22:00 to 7×10^{13} molecules cm^{-3} at midnight. This predicted concentration is likely much higher than that in Pittsburgh. For example, the Environmental Protection Agency Photochemical Assessment Monitoring Station in Pittsburgh measured concentrations of propylene during the summer of 2023, with a maximum observed concentration of 8×10^{10} molecules cm^{-3}.[57] Older studies from Pittsburgh have presented the maximum ethylene concentration of 3×10^{10} molecules cm^{-3},[58] propylene of 7×10^9 molecules cm^{-3},[59] and butene of 5×10^9 molecules cm^{-3}.[59] The highest alkene concentration observed in Beijing was ~4×10^{12} molecules cm^{-3}, and the concentration did not change by more than an order of magnitude on any night.[12] Alkene concentrations would have to be orders of magnitude higher than previously observed to compensate for the increased CS during events, so this analysis suggests that SO_2 oxidation by SCI is unlikely to explain the H_2SO_4 events.

https://doi.org/10.1021/acs.est.5c14137
Environ. Sci. Technol. XXXX, XXX, XXX–XXX

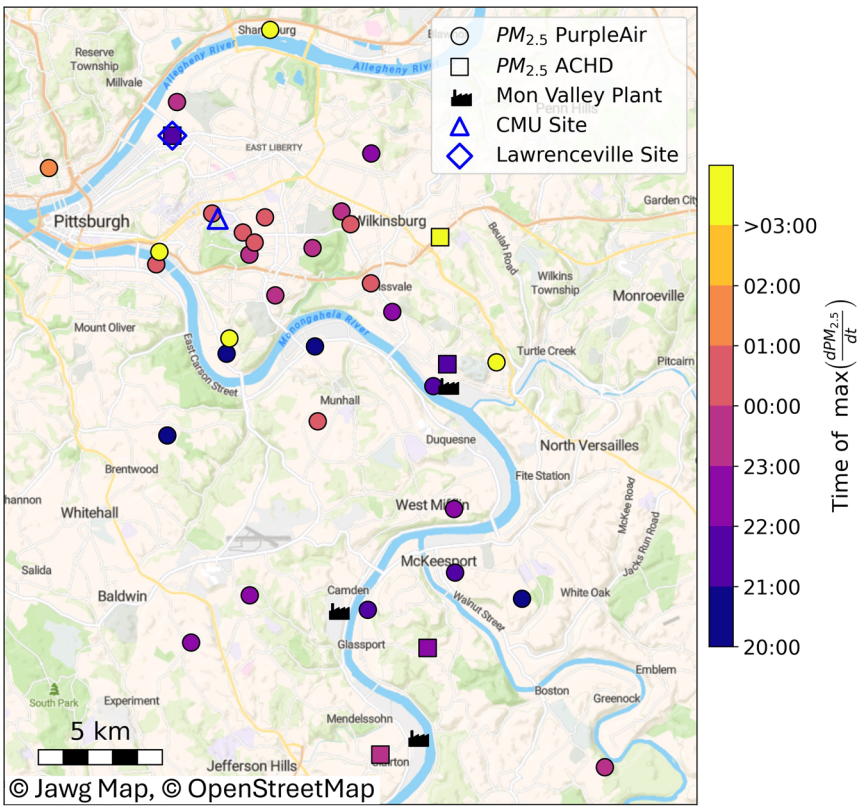

Figure 3. Map of Pittsburgh and its surrounding regions. Points are colored based upon the time of max increases in $PM_{2.5}$ between the hours of 20:00 and 07:00 on October 11th−12th, 2023. Circles are $PM_{2.5}$ measurements from PurpleAir sensors, and squares are from ACHD sensors. Map is reproduced with permission from Jawg Maps.

The strong positive correlation of SO_3 and H_2SO_4 concentrations with CS coupled with the sudden appearance of particles suggests that these compounds must be forming inside a particle-laden plume that travels to the measurement site at night. The wind velocity was used to determine where the plume was emitted. During the campaign, the wind speed was low (0.8−1.5 m s^{-1}) on both nonevent and event nights, further supporting the argument that the H_2SO_4 was not transported long distances. In addition, the nocturnal boundary layer consistently contracted after sunset to ∼100 m, which reduced the volume of the boundary layer and made local emissions more pronounced. On event nights, the wind direction measured at the Lawrenceville and North Braddock ACHD sites blew from the southeast while the Liberty ACHD sites measured a southerly wind direction. This contrasts with nonevent nights where the wind at Lawrenceville, North Braddock, and Liberty most often came from the north, east, and east northeast, respectively. The low wind speeds at night may affect measurements of wind direction, which have increased uncertainty when the air is calm.

To further pinpoint the source of the plume, PurpleAir $PM_{2.5}$ and ACHD $PM_{2.5}$ measurements were used to track the plume's movement through the region. $PM_{2.5}$ was used as it correlates with CS, H_2SO_4, and SO_3 (more details on this below). Figure 3 shows the hour when each $PM_{2.5}$ sensor first observed the air mass containing elevated $PM_{2.5}$ from October 11th to 12th, 2023. The timing corresponds to the one hour period with the largest increase in the $PM_{2.5}$ concentration at each sensor, excluding any sensors with a nightly maximum concentration less than 3 $\mu g\ m^{-3}$. Note, observations near Lawrenceville often increased earlier in the night than other $PM_{2.5}$ sensors in Pittsburgh, indicating that Lawrenceville may sample a different air mass or measure $PM_{2.5}$ from a hyperlocal source. In Figure 3, a large increase in $PM_{2.5}$ is observed near the MVW complex plants between 21:00 and 22:00 EDT, suggesting that this area is the source of the plume. The air mass then moved toward Pittsburgh, with sensors near CMU observing the largest increase in $PM_{2.5}$ between 23:00 and 01:00 EDT. This time aligns with the first H_2SO_4 event of the night (Figure 2), further supporting the conclusion that H_2SO_4 is from the plume. In addition, Gaussian plume models from Plume Pittsburgh show potential emissions from the MVW complex sites blowing toward Pittsburgh and reaching CMU between 23:00 and 23:59 EDT see Figure S7. The plume model also shows that the Lawrenceville site experienced the plume later than CMU did. The combined information from $PM_{2.5}$ measurements and plume modeling reveals that the air mass containing $PM_{2.5}$, H_2SO_4, and SO_3 comes from the region southeast of the measurement site where the MVW complex is located.

The Lawrenceville site contained additional instruments for gas and particulate composition that complement the measurements conducted at the CMU. In Figure 4, gas and particle phase measurements from the nights of October 11th−12th, 2023 (A−C) and October 12th−13th, 2024 (D−F) taken from both locations. To relate these measurements with those at CMU (Figure 4A and D), the plume was first confirmed to be present at both locations at the same time. Figure 4B and E displays the concentrations of $PM_{2.5}$ measured at CMU and Lawrenceville. As seen with the CS, the concentrations of $PM_{2.5}$ near CMU positively correlated with H_2SO_4 for both nights. The concentration of $PM_{2.5}$ in Lawrenceville increased

https://doi.org/10.1021/acs.est.5c14137
Environ. Sci. Technol. XXXX, XXX, XXX−XXX

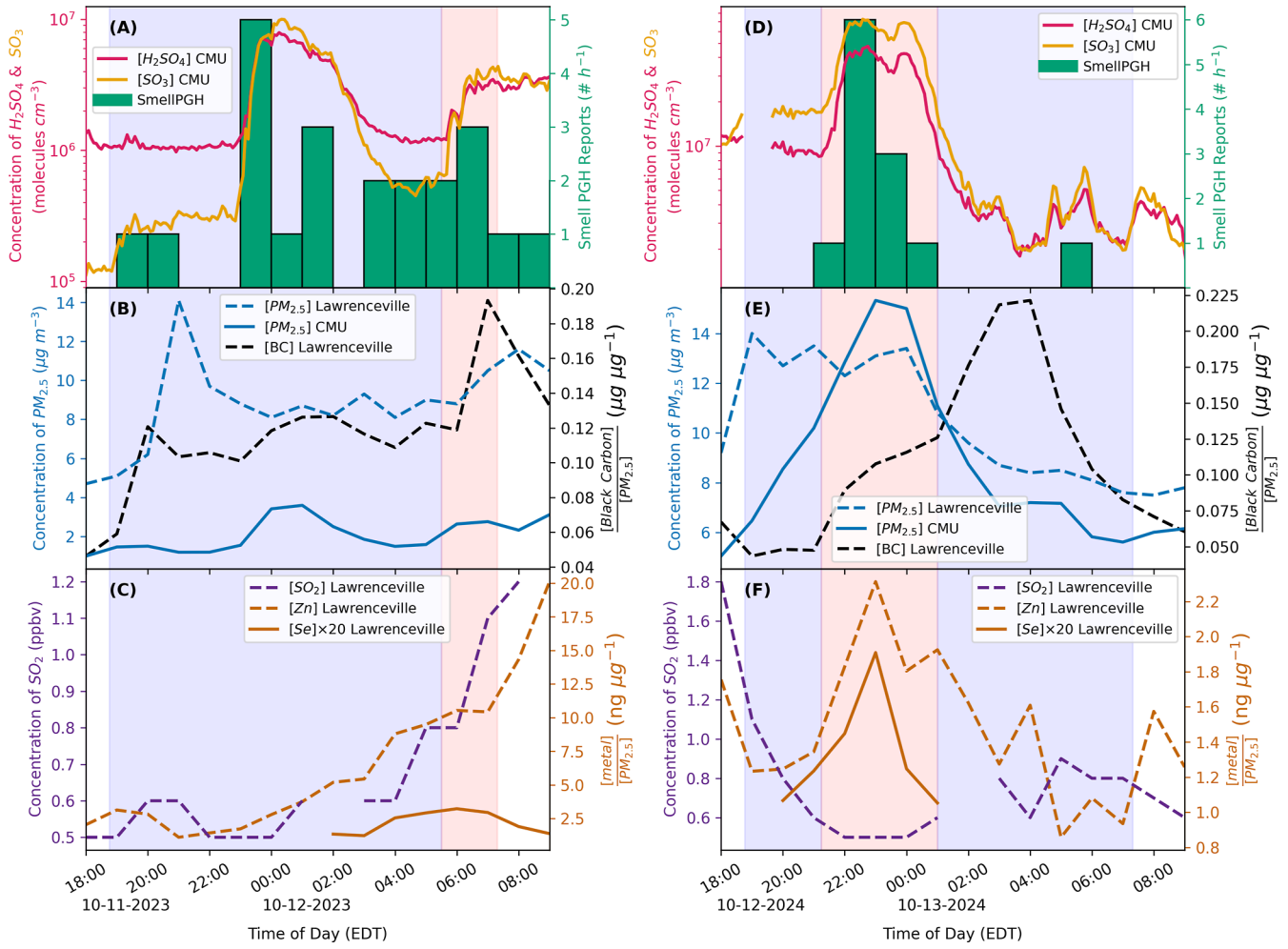

Figure 4. Measurements during two H_2SO_4 events on October 11th–12th, 2023 (A–C) and October 12th–13th, 2024 (D–F). H_2SO_4 and SO_3 were measured at CMU, and SmellPGH reports were from within Pittsburgh's city limits (A and D). Black carbon (BC) was observed at Lawrenceville, and $PM_{2.5}$ was measured at CMU and Lawrenceville (B and E). SO_2 concentration and mass fraction of metal to $PM_{2.5}$ were taken at Lawrenceville (C and F). The purple region indicates nighttime hours with the overlapping pink shaded region signifying times the plume was likely sampled at the CMU and Lawrenceville sites.

early in the night for both nights, likely due to hyperlocal sources, making it difficult to identify when the particle-filled plume reached Lawrenceville. However, the mass fraction of BC, a tracer for combustion emissions,[25,29] in Lawrenceville increased at 23:00 EDT on October 12th, 2024 (Figure 4E). This trend is also seen in the early morning (06:00) on October 12th, 2023 (Figure 4B), when the second H_2SO_4 event of the night is observed. It is likely that the CMU and Lawrenceville sites are both measuring the same air mass in the early morning of October 12th, 2023; however, it is obscured in Figure 3 by emissions from earlier in the night.

The strong correlation between H_2SO_4 and SO_3 with BC does not hold when the plume reaches the sites at different times. For example, between 23:00 and 00:00 EDT on October 11th to 12th, 2023 (Figure 4B), the $PM_{2.5}$ concentration and BC mass fraction do not clearly increase with the H_2SO_4 and SO_3 observed at CMU. Figure 3 and the plume modeling (Figure S7) demonstrate that the first plume reaches CMU at 00:00 EDT on October 12th, 2023; however, the plume model then shows that the plume trajectory changed direction before reaching Lawrenceville. A lower concentration of emissions may still reach Lawrenceville around 00:00 EDT on October 12th, which is consistent with the small increases in BC, $PM_{2.5}$, and metals at Lawrenceville. In addition, BC mass fraction and H_2SO_4 are anticorrelated on October 13th, 2024 between 01:00 and 02:00 EDT, during which the $PM_{2.5}$ concentration at both sites also decreases. The increase in BC mass fraction indicates a change in the particle emission source from the plume originating near the Mon Valley. This also resulted in a decrease in the formation of SO_3 and H_2SO_4 at the CMU.

To better constrain the source of the plume, particulate metals measured at Lawrenceville were examined during periods when the plume reached CMU and Lawrenceville. As shown in Figures 4C and F and S9, mass fractions of Zn, Se, Fe, and Mn were observed to increase during the events on October 11th–12th, 2023, and October 12th–13th, 2024. This further indicates emissions from coal burning, as all three metals can be emitted by coal combustion.[30−32,60] Similar to BC, the correlation of metal mass fraction with the H_2SO_4 concentration (Figure S10) varied widely depending on the night, likely a result of Xact and CIMS measuring different air masses.

The combined observations across these two sites demonstrate two important points: (1) Lawrenceville measured the same air plume as CMU at 06:00 on October 12th,

https://doi.org/10.1021/acs.est.5c14137
Environ. Sci. Technol. XXXX, XXX, XXX−XXX

2023, and 22:00 on October 12th, 2024, as the sites observed a simultaneous increase in BC, metals, $PM_{2.5}$, H_2SO_4, and SO_3 and (2) the plume originated from coal combustion sources. This further supports that the plume was emitted from the region with the MVW complex, where the coke plant, steel mill, and steel processing plant are known producers of high concentrations of $PM_{2.5}$, BC, and trace metals.[32,33,60,61]

The production of SO_3 and H_2SO_4 requires precursor gases of either SO_2 and/or H_2S. Figure 4A and D demonstrates that the timelines of SmellPGH reports across the city correlate with increases in concentrations of H_2SO_4 and SO_3. All SmellPGH reports originate from users in Pittsburgh who self-report unpleasant smells or bad air quality. Of the SmellPGH reports, 24% contained optional keywords related to the smell of sulfur (e.g., rotten eggs, brimstone, and sewage). The sulfur smells reported are more likely H_2S than SO_2, as the smell of H_2S is recognizable at five ppbv, while SO_2 is not detectable by smell until one ppmv.[62,63] Methanethiol is another potential sulfur-smelling compound; however, this compound has not previously been reported as an emission from steel production or coke works. In addition, the ACHD North Braddock and Liberty sites, see Figure S1 for locations, measured nocturnal H_2S concentrations up to 20 ppbv (10/11/2024) and 52 ppbv (10/1/2023), respectively, when the plume traveled toward these ACHD sites instead of northwest to CMU. These observations indicate that the plumes contain high concentrations of H_2S. As such, the H_2SO_4 and SO_3 events are likely linked to an increase in H_2S concentrations.

Concentrations of SO_2, the key precursor for H_2SO_4 and SO_3, measured in Lawrenceville are shown in Figure 4C and F. The concentration of SO_2 remained low during both campaigns. Most nightly maxima fall below one ppbv, lower than the median SO_2 concentration of two ppbv observed during nocturnal events in Beijing.[12,21] Beijing events saw a positive correlation between SO_2, H_2SO_4, and SO_3, indicating SO_2 oxidation is the source of nighttime SO_3 and H_2SO_4 formation. During Pittsburgh campaigns, the median correlation between nightly SO_2 and H_2SO_4 concentrations, displayed in Figure S4, was 0.10 for the event nights. The weak correlation may be due to differences in the air masses at the different sampling locations, an unidentified limiting reagent in the oxidation processes, or a combination of both. During the event on October 12th, 2024, when both CMU and Lawrenceville are expected to sample the same air mass, the correlation between SO_2 and H_2SO_4 was negative, suggesting that low concentrations of SO_2 (~0.5 ppbv) do not limit the nocturnal formation of H_2SO_4. Measurements of SO_2 concentration collocated with H_2SO_4 are needed to rule out the impacts of location and dilution on the measurements, as the insensitivity to SO_2 concentration contrasts with previous observations of nocturnal H_2SO_4 formation.[12,21]

In a study by Yuo et al., the formation of nocturnal SO_3 was explained by the heterogeneous catalysis of SO_2 on the surface of BC aerosol particles. They observed a positive correlation between concentrations of SO_3 and the product of SO_2 and BC concentrations ($[SO_2]\times[BC]$). To examine if this is a potential nighttime H_2SO_4 and SO_3 formation pathway for Pittsburgh, $[SO_2] \times [BC]$ were correlated to the concentrations of SO_3 and H_2SO_4 (Figure S4). For event nights, there was no overall correlation as the median correlation was 0.03. During some time periods, such as 06:00 on October 12th, 2023, SO_2, BC, H_2SO_4, and SO_3 all increased at the same time. However, the overall correlation of $[SO_2] \times [BC]$ for October 11th to 12th, 2023 was 0.03 as it did not correlate with the first H_2SO_4 event of the night. Measurement of BC and SO_2 at CMU would likely improve the correlation but may not explain all events due to low SO_2 concentrations when both sites measured the same air mass, as discussed previously. As such, catalytic formation of H_2SO_4 from BC and SO_2 does not seem to be the dominant pathway for nocturnal H_2SO_4 formation in the steel and coal emission plume.

In addition to BC, metal oxides have been shown to act as catalysts for the heterogeneous oxidation of SO_2 and H_2S and are used in the industrial production of H_2SO_4.[64−68] A wide range of metal oxides can act as catalysts, including oxides of Fe, Mn, and Zn.[64,65,67−69] Although the Xact is not able to measure the oxidation state, these metals were observed during events (Figures 4 and S9) and have previously been observed to exist in high concentrations as oxides in submicron coal combustion particles.[31,67,70] In addition, mixtures of these metal oxides, which have been identified in emissions from steel making, may be more effective at oxidizing SO_2 than oxides containing one type of metal.[70] Oxidation of H_2S may help explain the events, as concentrations of SO_2 measured in Lawrenceville were low, with most nights below one ppbv. The coke plant and steel mill are known to emit H_2S, and Pittsburgh residents frequently report smells associated with H_2S during the night.

Although not previously observed in field measurements, oxidation reactions catalyzed by metal oxides can occur at ambient conditions, with laboratory measurements of oxidation of H_2S and SO_2 observed at room temperature on a ternary metal oxide containing nanoparticles of Fe, Mn, and Zn.[66] However, the oxidation of sulfur compounds on the ternary metal oxides did not observe desorption of the product from the oxide surface to the gas phase, which has a high activation energy at low temperatures.[65] For aerosols containing metal oxides, the size and curvature of the particles may decrease the energy required for desorption, resulting in more desorption from the aerosol surface at a lower temperature. These effects are dependent on the adsorbed molecule, catalyst composition, particle size, and temperature.[71−73] Other properties of the aerosol may enhance the oxidation rate, such as the presence of binary metal oxides, higher concentrations of metals at the surface of the coal combustion particle, and a higher concentration of reaction sites compared to bulk.[64,74,75] To determine the oxidation state of the metals, samples of $PM_{2.5}$ should be examined by X-ray photoelectron spectroscopy.[76] Computation chemistry studies, similar to those done for SO_2 and BC aerosols,[25] may help identify if the adsorption, oxidation, and desorption of H_2S and SO_2 on metal oxide aerosols is a feasible nocturnal formation pathway for SO_3 and H_2SO_4 at atmospheric conditions.

Another family of compounds that may enhance the oxidation of sulfur molecules are reactive nitrogen compounds (e.g., NO_x, NO_z, and HONO), which can be emitted by coal combustion and steelmaking.[77−79] NO_x concentrations measured in Lawrenceville showed a strong correlation during event nights when the plume reached CMU and Lawrenceville, such as on October 12th−13th, 2024 with an observed correlation of 0.79. In addition, nitrate (NO_3^-, formed from hydrolysis of N_2O_5 at night)[80] has previously been shown to improve uptake and accelerate oxidation of SO_2 on Fe_2O_3 at ambient temperatures and in the absence of solar radiation.[81] The CIMS also observed 93.00, 108.99, and 140.98 amu to correlate with H_2SO_4 and SO_3 (correlation values of 0.50, 0.42,

https://doi.org/10.1021/acs.est.5c14137
Environ. Sci. Technol. XXXX, XXX, XXX−XXX

and 0.49 during event nights, Figure S11). Though definitive identification of these peaks is challenging, the masses and isotope ratios correspond to nitrogen oxides, specifically $HNO{\cdot}NO_3^-$, $HONO{\cdot}NO_3^-$, and $HNO_4{\cdot}NO_3^-$, see the Supporting Information for more discussion. The increase of HONO-related masses could also be explained by nitrate enhancement of SO_2 on Fe_2O_3 as the process was previously found to form HONO.[81] The strong correlation of the reactive nitrogen compounds could suggest that reactive nitrogen compounds emitted from coal combustion and steelmaking may enhance the uptake of SO_2 onto metal oxides and accelerate the oxidation of SO_2 into SO_3 and H_2SO_4.

Overall, measurements and models conducted during the campaigns show air masses on H_2SO_4 event nights originating from the southeast of Pittsburgh near the MVW complex. The air plumes are likely emissions from the steel industry, as these plants are the largest emitters in that area. The H_2SO_4 events occurred on a local scale with the different parts of Pittsburgh observing the plume at different times. The measured air mass contained elevated BC and trace metal concentrations, further suggesting that they contain emissions from combustion. Previous studies suggest that metal oxides and BC could heterogeneously oxidize H_2S and SO_2 into SO_3 and H_2SO_4. Observations of the polluted air masses in Pittsburgh demonstrate that metal oxides, such as those from Fe, Mn, Zn, and BC are present in the aerosol particles and correlate well with H_2SO_4 events. In addition, the very high correlation of H_2SO_4 and SO_3 with reactive nitrogen compounds (e.g., HONO) suggests that these compounds could potentially accelerate the uptake and oxidation of SO_2 with Fe_2O_3 on the surface of aerosol particles. These observations of nocturnal SO_3 and H_2SO_4 in Pittsburgh demonstrate previously unobserved chemistry occurring in the emissions from coal burning or steel production. More laboratory and collocated field measurements are needed to quantify the various potential reaction pathways and identify key compounds in the nighttime oxidation of sulfur species to SO_3 and H_2SO_4 within the emissions plume.

■ ASSOCIATED CONTENT

Data Availability Statement

Measurements from the CMU site are available at 10.1184/R1/30577211. Data from the ACHD is available on the Western Pennsylvania Regional Data Center (https://data.wprdc.org/dataset/allegheny-county-air-quality). PurpleAir measurements can be downloaded using the PurpleAir api (https://api.purpleair.com/). Measurements from ASCENT will be available in the future on their own database, see https://ascent.research.gatech.edu/database for more information. Plume Pittsburgh and SmellPGH are available through the CMU Create Lab (https://www.cmucreatelab.org/projects).

Supporting Information

The Supporting Information is available free of charge at https://pubs.acs.org/doi/10.1021/acs.est.5c14137.

Further descriptions of measurement sites, CIMS, nonevent night timelines, nightly correlations of H_2SO_4, H_2SO_4 24 h timeline, Plume Pittsburgh Gaussian Plume Models of MVW emissions, Xact $PM_{2.5}$ metal composition, and CIMS m/z ratios correlated with H_2SO_4 (PDF)

■ AUTHOR INFORMATION

Corresponding Author

Coty N. Jen − *Department of Chemical Engineering, Carnegie Mellon University, Pittsburgh, Pennsylvania 15213, United States; Center for Atmospheric Particle Studies, Carnegie Mellon University, Pittsburgh, Pennsylvania 15213, United States;* orcid.org/0000-0002-3633-4614; Email: cotyj@andrew.cmu.com

Authors

Dominic A. Casalnuovo − *Department of Chemical Engineering, Carnegie Mellon University, Pittsburgh, Pennsylvania 15213, United States; Center for Atmospheric Particle Studies, Carnegie Mellon University, Pittsburgh, Pennsylvania 15213, United States;* orcid.org/0000-0003-4782-6953

Darren Cheng − *Center for Atmospheric Particle Studies and Department of Mechanical Engineering, Carnegie Mellon University, Pittsburgh, Pennsylvania 15213, United States*

Christine Troller − *Department of Chemical Engineering, Carnegie Mellon University, Pittsburgh, Pennsylvania 15213, United States; Center for Atmospheric Particle Studies, Carnegie Mellon University, Pittsburgh, Pennsylvania 15213, United States;* orcid.org/0009-0005-3588-8315

Ziheng Zeng − *Department of Chemical Engineering, Carnegie Mellon University, Pittsburgh, Pennsylvania 15213, United States; Center for Atmospheric Particle Studies, Carnegie Mellon University, Pittsburgh, Pennsylvania 15213, United States*

Albert A. Presto − *Center for Atmospheric Particle Studies and Department of Mechanical Engineering, Carnegie Mellon University, Pittsburgh, Pennsylvania 15213, United States*

Complete contact information is available at: https://pubs.acs.org/10.1021/acs.est.5c14137

Notes

The authors declare no competing financial interest.

■ ACKNOWLEDGMENTS

The DAC, DC, CT, ZZ, and CNJ acknowledge support from DOE ASR DE-SC0022224. DAC was supported by NSF GRFP (DGE2140739). Funding for ASCENT was provided by NSF AGS-2131914. The authors would like to acknowledge the Allegheny County Health Department for their measurements, CMU Create Lab for their development of Smell Pittsburgh and Plume Pittsburgh, and PurpleAir for their contribution to science by making data publicly available.

■ REFERENCES

(1) Gordon, H.; Kirkby, J.; Baltensperger, U.; Bianchi, F.; Breitenlechner, M.; Curtius, J.; Dias, A.; Dommen, J.; Donahue, N. M.; Dunne, E. M.; Duplissy, J.; Ehrhart, S.; Flagan, R. C.; Frege, C.; Fuchs, C.; Hansel, A.; Hoyle, C. R.; Kulmala, M.; Kürten, A.; Lehtipalo, K.; Makhmutov, V.; Molteni, U.; Rissanen, M. P.; Stozkhov, Y.; Tröstl, J.; Tsagkogeorgas, G.; Wagner, R.; Williamson, C.; Wimmer, D.; Winkler, P. M.; Yan, C.; Carslaw, K. S. Causes and Importance of New Particle Formation in the Present-Day and Preindustrial Atmospheres. *J. Geophys. Res.:Atmos.* **2017**, *122* (16), 8739−8760.

(2) Spracklen, D. V.; Carslaw, K. S.; Kulmala, M.; Kerminen, V.-M.; Mann, G. W.; Sihto, S.-L. The Contribution of Boundary Layer Nucleation Events to Total Particle Concentrations on Regional and Global Scales. *Atmos. Chem. Phys.* **2006**, *6* (12), 5631−5648.

(3) Merikanto, J.; Spracklen, D. V.; Mann, G. W.; Pickering, S. J.; Carslaw, K. S. Impact of Nucleation on Global CCN. *Atmos. Chem. Phys.* **2009**, *9* (21), 8601−8616.
(4) Hidy, G. M.; Katz, J. L.; Mirabel, P. Sulfate Aerosol Formation and Growth in the Stratosphere. *Atmos Environ* **1978**, *12* (4), 887−892.
(5) Yue, D. L.; Hu, M.; Zhang, R. Y.; Wang, Z. B.; Zheng, J.; Wu, Z. J.; Wiedensohler, A.; He, L. Y.; Huang, X. F.; Zhu, T. The Roles of Sulfuric Acid in New Particle Formation and Growth in the Mega-City of Beijing. *Atmos. Chem. Phys.* **2010**, *10* (10), 4953−4960.
(6) Spracklen, D. V.; Carslaw, K. S.; Kulmala, M.; Kerminen, V.-M.; Sihto, S.-L.; Riipinen, I.; Merikanto, J.; Mann, G. W.; Chipperfield, M. P.; Wiedensohler, A.; Birmili, W.; Lihavainen, H. Contribution of Particle Formation to Global Cloud Condensation Nuclei Concentrations. *Geophys. Res. Lett.* **2008**, *35*(6)..
(7) Chen, M.; Titcombe, M.; Jiang, J.; Jen, C.; Kuang, C.; Fischer, M. L.; Eisele, F. L.; Siepmann, J. I.; Hanson, D. R.; Zhao, J.; McMurry, P. H. Acid−Base Chemical Reaction Model for Nucleation Rates in the Polluted Atmospheric Boundary Layer. *Proc. Natl. Acad. Sci. U.S.A.* **2012**, *109* (46), 18713−18718.
(8) Kuang, C.; McMurry, P. H.; McCormick, A. V.; Eisele, F. L. Dependence of Nucleation Rates on Sulfuric Acid Vapor Concentration in Diverse Atmospheric Locations. *J. Geophys. Res.:Atmos.* **2008**, *113*(D10)..
(9) Weber, R. J.; Marti, J. J.; McMurry, P. H.; Eisele, F. L.; Tanner, D. J.; Jefferson, A. Measured Atmospheric New Particle Formation Rates: Implications for Nucleation Mechanisms. *Chem. Eng. Commun.* **1996**, *151*, 53−64.
(10) Lu, Y.; Yan, C.; Fu, Y.; Chen, Y.; Liu, Y.; Yang, G.; Wang, Y.; Bianchi, F.; Chu, B.; Zhou, Y.; Yin, R.; Baalbaki, R.; Garmash, O.; Deng, C.; Wang, W.; Liu, Y.; Petäjä, T.; Kerminen, V.-M.; Jiang, J.; Kulmala, M.; Wang, L. A Proxy for Atmospheric Daytime Gaseous Sulfuric Acid Concentration in Urban Beijing. *Atmos. Chem. Phys.* **2019**, *19* (3), 1971−1983.
(11) Mikkonen, S.; Romakkaniemi, S.; Smith, J. N.; Korhonen, H.; Petäjä, T.; Plass-Duelmer, C.; Boy, M.; McMurry, P. H.; Lehtinen, K. E. J.; Joutsensaari, J.; Hamed, A.; Mauldin III, R. L.; Birmili, W.; Spindler, G.; Arnold, F.; Kulmala, M.; Laaksonen, A. A Statistical Proxy for Sulphuric Acid Concentration. *Atmos. Chem. Phys.* **2011**, *11* (21), 11319−11334.
(12) Guo, Y.; Yan, C.; Li, C.; Ma, W.; Feng, Z.; Zhou, Y.; Lin, Z.; Dada, L.; Stolzenburg, D.; Yin, R.; Kontkanen, J.; Daellenbach, K. R.; Kangasluoma, J.; Yao, L.; Chu, B.; Wang, Y.; Cai, R.; Bianchi, F.; Liu, Y.; Kulmala, M. Formation of Nighttime Sulfuric Acid from the Ozonolysis of Alkenes in Beijing. *Atmos. Chem. Phys.* **2021**, *21* (7), 5499−5511.
(13) Lelieveld, J.; Butler, T. M.; Crowley, J. N.; Dillon, T. J.; Fischer, H.; Ganzeveld, L.; Harder, H.; Lawrence, M. G.; Martinez, M.; Taraborrelli, D.; Williams, J. Atmospheric Oxidation Capacity Sustained by a Tropical Forest. *Nature* **2008**, *452* (7188), 737−740.
(14) Alicke, B.; Geyer, A.; Hofzumahaus, A.; Holland, F.; Konrad, S.; Pätz, H. W.; Schäfer, J.; Stutz, J.; Volz-Thomas, A.; Platt, U. OH Formation by HONO Photolysis during the BERLIOZ Experiment. *J. Geophys. Res.:Atmos.* **2003**, *108*(D4), PHO 3−1-PHO 3−17. DOI: .
(15) Whalley, L. K.; Furneaux, K. L.; Goddard, A.; Lee, J. D.; Mahajan, A.; Oetjen, H.; Read, K. A.; Kaaden, N.; Carpenter, L. J.; Lewis, A. C.; Plane, J. M. C.; Saltzman, E. S.; Wiedensohler, A.; Heard, D. E. The Chemistry of OH and HO_2 Radicals in the Boundary Layer over the Tropical Atlantic Ocean. *Atmos. Chem. Phys.* **2010**, *10* (4), 1555−1576.
(16) Lovejoy, E. R.; Hanson, D. R.; Huey, L. G. Kinetics and Products of the Gas-Phase Reaction of SO3 with Water. *J. Phys. Chem.* **1996**, *100* (51), 19911−19916.
(17) Bandyopadhyay, B.; Kumar, P.; Biswas, P. Ammonia Catalyzed Formation of Sulfuric Acid in Troposphere: The Curious Case of a Base Promoting Acid Rain. *J. Phys. Chem. A* **2017**, *121* (16), 3101−3108.
(18) Long, B.; Chang, C.-R.; Long, Z.-W.; Wang, Y.-B.; Tan, X.-F.; Zhang, W.-J. Nitric Acid Catalyzed Hydrolysis of SO3 in the Formation of Sulfuric Acid: A Theoretical Study. *Chem. Phys. Lett.* **2013**, *581*, 26−29.
(19) Lv, G.; Sun, X.; Zhang, C.; Li, M. Understanding the Catalytic Role of Oxalic Acid in SO_3 Hydration to Form H_2SO_4 in the Atmosphere. *Atmos. Chem. Phys.* **2019**, *19* (5), 2833−2844.
(20) Boy, M.; Mogensen, D.; Smolander, S.; Zhou, L.; Nieminen, T.; Paasonen, P.; Plass-Dülmer, C.; Sipilä, M.; Petäjä, T.; Mauldin, L.; Berresheim, H.; Kulmala, M. Oxidation of SO2 by Stabilized Criegee Intermediate (sCI) Radicals as a Crucial Source for Atmospheric Sulfuric Acid Concentrations. *Atmos. Chem. Phys.* **2013**, *13* (7), 3865−3879.
(21) Yao, L.; Fan, X.; Yan, C.; Kurtén, T.; Daellenbach, K. R.; Li, C.; Wang, Y.; Guo, Y.; Dada, L.; Rissanen, M. P.; Cai, J.; Tham, Y. J.; Zha, Q.; Zhang, S.; Du, W.; Yu, M.; Zheng, F.; Zhou, Y.; Kontkanen, J.; Chan, T.; Shen, J.; Kujansuu, J. T.; Kangasluoma, J.; Jiang, J.; Wang, L.; Worsnop, D. R.; Petäjä, T.; Kerminen, V.-M.; Liu, Y.; Chu, B.; He, H.; Kulmala, M.; Bianchi, F. Unprecedented Ambient Sulfur Trioxide (SO3) Detection: Possible Formation Mechanism and Atmospheric Implications. *Environ. Sci. Technol. Lett.* **2020**, *7* (11), 809−818.
(22) Mauldin, R. L., III; Berndt, T.; Sipilä, M.; Paasonen, P.; Petäjä, T.; Kim, S.; Kurtén, T.; Stratmann, F.; Kerminen, V.-M.; Kulmala, M. A New Atmospherically Relevant Oxidant of Sulphur Dioxide. *Nature* **2012**, *488* (7410), 193−196.
(23) Chao, W.; Hsieh, J.-T.; Chang, C.-H.; Lin, J. J.-M. Direct Kinetic Measurement of the Reaction of the Simplest Criegee Intermediate with Water Vapor. *Science* **2015**, *347* (6223), 751−754.
(24) Long, B.; Bao, J. L.; Truhlar, D. G. Rapid Unimolecular Reaction of Stabilized Criegee Intermediates and Implications for Atmospheric Chemistry. *Nat. Commun.* **2019**, *10* (1), 2003.
(25) He, G.; Ma, J.; He, H. Role of Carbonaceous Aerosols in Catalyzing Sulfate Formation. *ACS Catal.* **2018**, *8* (5), 3825−3832.
(26) Byrwa-Hill, B. M.; Presto, A. A.; Wenzel, S.; Fabisiak, J. P. Impact of a Pollution Breach at a Coke Oven Factory on Asthma Control in Nearby Vulnerable Adults. *J. Allergy Clin. Immunol.* **2021**, *148* (1), 225−233.
(27) Emissions Inventory. https://www.alleghenycounty.us/Services/Health-Department/Air-Quality/Air-Quality-Dashboards/Emissions-Inventory (accessed Jun 18, 2025).
(28) ACHD. *Analysis and Attribution of Hydrogen Sulfide (H2S) Exceedances at the Liberty Monitoring Site from January 1, 2020 through March 1, 2022*; Allegheny County Health Department Air Quality Program, 2022. https://www.alleghenycounty.us/files/assets/county/v/1/government/health/documents/air-quality/h2s_report_updated_08052022.pdf (accessed Jun 18, 2025).
(29) Blanco-Alegre, C.; Fialho, P.; Calvo, A. I.; Castro, A.; Coz, E.; Oduber, F.; Prévôt, A. S. H.; Močnik, G.; Alves, C.; Giardi, F.; Pazzi, G.; Fraile, R. Contribution of Coal Combustion to Black Carbon: Coupling Tracers with the Aethalometer Model. *Atmos. Res.* **2022**, *267*, 105980.
(30) Sambandam, B.; Devasena, T.; Islam, V. I. H.; Prakhya, B. M. Characterization of Coal Fly Ash Nanoparticles and Their Induced in Vitro Cellular Toxicity and Oxidative DNA Damage in Different Cell Lines. *Indian J. Exp. Biol.* **2015**, *53* (9), 585−593.
(31) Amdur, M. O.; Sarofim, A. F.; Neville, M.; Quann, R. J.; McCarthy, J. F.; Elliott, J. F.; Lam, H. F.; Rogers, A. E.; Conner, M. W. Coal Combustion Aerosols and Sulfur Dioxide: An Interdisciplinary Analysis. *Environ. Sci. Technol.* **1986**, *20* (2), 138−145.
(32) Laden, F.; Neas, L. M.; Dockery, D. W.; Schwartz, J. Association of Fine Particulate Matter from Different Sources with Daily Mortality in Six U.S. Cities. *Environ. Health Perspect.* **2000**, *108*, 941.
(33) Tunno, B. J.; Michanowicz, D. R.; Shmool, J. L. C.; Kinnee, E.; Cambal, L.; Tripathy, S.; Gillooly, S.; Roper, C.; Chubb, L.; Clougherty, J. E. Spatial Variation in Inversion-Focused vs 24-h Integrated Samples of PM2.5 and Black Carbon across Pittsburgh, PA. *J. Expo Sci. Environ. Epidemiol* **2016**, *26* (4), 365−376.
(34) Fomete, S. K. W.; Johnson, J. S.; Myllys, N.; Jen, C. N. Experimental and Theoretical Study on the Enhancement of

https://doi.org/10.1021/acs.est.5c14137
Environ. Sci. Technol. XXXX, XXX, XXX−XXX

Alkanolamines on Sulfuric Acid Nucleation. *J. Phys. Chem. A* **2022**, *126* (25), 4057−4067.
(35) Zhao, J.; Eisele, F. L.; Titcombe, M.; Kuang, C.; McMurry, P. H. Chemical Ionization Mass Spectrometric Measurements of Atmospheric Neutral Clusters Using the Cluster-CIMS. *J. Geophys. Res.:Atmos.* **2010**, *115*(D8)..
(36) Zhao, J.; Smith, J. N.; Eisele, F. L.; Chen, M.; Kuang, C.; McMurry, P. H. Observation of Neutral Sulfuric Acid-Amine Containing Clusters in Laboratory and Ambient Measurements. *Atmos. Chem. Phys.* **2011**, *11* (21), 10823−10836.
(37) Jen, C. N.; Zhao, J.; McMurry, P. H.; Hanson, D. R. Chemical Ionization of Clusters Formed from Sulfuric Acid and Dimethylamine or Diamines. *Atmos. Chem. Phys.* **2016**, *16*, 12513−12529.
(38) Yin, K.; Mai, S.; Zhao, J. Atmospheric Sulfuric Acid Dimer Formation in a Polluted Environment. *Int. J. Environ. Res. Public Health* **2022**, *19* (11), 6848.
(39) Berresheim, H.; Elste, T.; Plass-Dülmer, C.; Eiseleb, F. L.; Tannerb, D. J. Chemical Ionization Mass Spectrometer for Long-Term Measurements of Atmospheric OH and H_2SO_4. *Int. J. Mass Spectrom.* **2000**, *202*, 91−109.
(40) Viggiano, A. A.; Perry, R. A.; Albritton, D. L.; Ferguson, E. E.; Fehsenfeld, F. C. STRATOSPHERIC NEGATIVE-ION REACTION RATES WITH H2SO4. *J. Geophys. Res.* **1982**, *87*, 7340−7342.
(41) Arnold, S. T.; Morris, R. A.; Viggiano, A. A.; Jayne, J. T. Ion Chemistry Relevant for Chemical Ionization Detection of SO3. *J. Geophys. Res.:Atmos.* **1995**, *100* (D7), 14141−14146.
(42) Heinritzi, M.; Simon, M.; Steiner, G.; Wagner, A. C.; Kürten, A.; Hansel, A.; Curtius, J. Characterization of the Mass-Dependent Transmission Efficiency of a CIMS. *Atmos. Meas. Technol.* **2016**, *9* (4), 1449−1460.
(43) Hanson, D. R. Mass Accommodation of H2SO4 and CH3SO3H on Water−Sulfuric Acid Solutions from 6% to 97% RH. *J. Phys. Chem. A* **2005**, *109* (31), 6919−6927.
(44) Pöschl, U.; Canagaratna, M.; Jayne, J. T.; Molina, L. T.; Worsnop, D. R.; Kolb, C. E.; Molina, M. J. Mass Accommodation Coefficient of H_2SO_4 Vapor on Aqueous Sulfuric Acid Surfaces and Gaseous Diffusion Coefficient of H_2SO_4 in N_2/H_2O. *J. Phys. Chem. A* **1998**, *102* (49), 10082−10089.
(45) Cai, R.; Yang, D.; Fu, Y.; Wang, X.; Li, X.; Ma, Y.; Hao, J.; Zheng, J.; Jiang, J. Aerosol Surface Area Concentration: A Governing Factor in New Particle Formation in Beijing. *Atmos. Chem. Phys.* **2017**, *17* (20), 12327−12340.
(46) McMurry, P. H.; Fink, M.; Sakurai, H.; Stolzenburg, M. R.; Mauldin, R. L.; Smith, J.; Eisele, F.; Moore, K.; Sjostedt, S.; Tanner, D.; Huey, L. G.; Nowak, J. B.; Edgerton, E.; Voisin, D. A Criterion for New Particle Formation in the Sulfur-Rich Atlanta Atmosphere. *J. Geophys. Res.:Atmos.* **2005**, *110*(D22)..
(47) Kuang, C.; Riipinen, I.; Sihto, S.-L.; Kulmala, M.; McCormick, A. V.; McMurry, P. H. An Improved Criterion for New Particle Formation in Diverse Atmospheric Environments. *Atmos. Chem. Phys.* **2010**, *10* (17), 8469−8480.
(48) McMurry, P. H. New Particle Formation in the Presence of an Aerosol: Rates, Time Scales, and Sub-0.01 Mm Size Distributions. *J. Colloid Interface Sci.* **1983**, *95* (1), 72−80.
(49) Cheng, D.; Amanatidis, S.; Lewis, G. S.; Jen, C. N. Fast and Sensitive Measurements of Sub-3 Nm Particles Using Condensation Particle Counters For Atmospheric Rapid Measurements (CPC FARM). *Atmos. Meas. Tech.* **2025**, *18* (1), 197−210.
(50) Hass-Mitchell, T.; Joo, T.; Rogers, M.; Nault, B. A.; Soong, C.; Tran, M.; Seo, M.; Machesky, J. E.; Canagaratna, M.; Roscioli, J.; Claflin, M. S.; Lerner, B. M.; Blomdahl, D. C.; Misztal, P. K.; Ng, N. L.; Dillner, A. M.; Bahreini, R.; Russell, A.; Krechmer, J. E.; Lambe, A.; Gentner, D. R. Increasing Contributions of Temperature-Dependent Oxygenated Organic Aerosol to Summertime Particulate Matter in New York City. *ACS EST Air* **2024**, *1* (2), 113−128.
(51) Joo, T.; Rogers, M. J.; Soong, C.; Hass-Mitchell, T.; Heo, S.; Bell, M. L.; Ng, N. L.; Gentner, D. R. Aged and Obscured Wildfire Smoke Associated with Downwind Health Risks. *Environ. Sci. Technol. Lett.* **2024**, *11* (12), 1340−1347.
(52) Li, D.; Wu, Y.; Gross, B.; Moshary, F. Dynamics of Mixing Layer Height and Homogeneity from Ceilometer-Measured Aerosol Profiles and Correlation to Ground Level PM2.5 in New York City. *Remote Sens.* **2022**, *14* (24), 6370.
(53) Lee, J.; Hong, J.-W.; Lee, K.; Hong, J.; Velasco, E.; Lim, Y. J.; Lee, J. B.; Nam, K.; Park, J. Ceilometer Monitoring of Boundary-Layer Height and Its Application in Evaluating the Dilution Effect on Air Pollution. *Boundary-Layer Meteorol* **2019**, *172* (3), 435−455.
(54) The CREATE Lab. Smell Pittsburgh, 2018. https://smellpgh.org/(accessed 04 03, 2025).
(55) PurpleAir. https://www2.purpleair.com/(accessed 04 03, 2025).
(56) The CREATE Lab. Plume Pittsburgh, 2021. https://plumepgh.org/(accessed 04 03, 2025).
(57) PAMS Dashboard. https://rstudio-connect.sonomatechdata.com/pams_dashboard/(accessed Jun 19, 2025).
(58) Swarthout, R. F.; Russo, R. S.; Zhou, Y.; Miller, B. M.; Mitchell, B.; Horsman, E.; Lipsky, E.; McCabe, D. C.; Baum, E.; Sive, B. C. Impact of Marcellus Shale Natural Gas Development in Southwest Pennsylvania on Volatile Organic Compound Emissions and Regional Air Quality. *Environ. Sci. Technol.* **2015**, *49* (5), 3175−3184.
(59) Millet, D. B.; Donahue, N. M.; Pandis, S. N.; Polidori, A.; Stanier, C. O.; Turpin, B. J.; Goldstein, A. H. Atmospheric Volatile Organic Compound Measurements during the Pittsburgh Air Quality Study: Results, Interpretation, and Quantification of Primary and Secondary Contributions. *J. Geophys. Res.:Atmos.* **2005**, *110*(D7)..
(60) Weitkamp, E. A.; Lipsky, E. M.; Pancras, P. J.; Ondov, J. M.; Polidori, A.; Turpin, B. J.; Robinson, A. L. Fine Particle Emission Profile for a Large Coke Production Facility Based on Highly Time-Resolved Fence Line Measurements. *Atmos. Environ.* **2005**, *39* (36), 6719−6733.
(61) Tunno, B. J.; Shields, K. N.; Lioy, P.; Chu, N.; Kadane, J. B.; Parmanto, B.; Pramana, G.; Zora, J.; Davidson, C.; Holguin, F.; Clougherty, J. E. Understanding Intra-Neighborhood Patterns in PM2.5 and PM10 Using Mobile Monitoring in Braddock, PA. *Environ. Health* **2012**, *11* (1), 76.
(62) McGinley, M. A.; McGinley, C. M. Comparison of Field Olfactometers in a Controlled Chamber Using Hydrogen Sulfide as the Test Odorant. *Water Sci. Technol.* **2004**, *50* (4), 75−82.
(63) Kleinbeck, S.; Schäper, M.; Juran, S. A.; Kiesswetter, E.; Blaszkewicz, M.; Golka, K.; Zimmermann, A.; Brüning, T.; Van Thriel, C. Odor Thresholds and Breathing Changes of Human Volunteers as Consequences of Sulphur Dioxide Exposure Considering Individual Factors. *Safety and Health at Work* **2011**, *2* (4), 355−364.
(64) Lowell, P. S.; Schwitzgebel, K.; Parsons, T. B.; Sladek, K. J. Selection of Metal Oxides for Removing SO_2 From Flue Gas. *Ind. Eng. Chem. Proc. Des. Dev.* **1971**, *10* (3), 384−390.
(65) Lapina, O. B.; Bal'zhinimaev, B. S.; Boghosian, S.; Eriksen, K. M.; Fehrmann, R. Progress on the Mechanistic Understanding of SO2 Oxidation Catalysts. *Catal. Today* **1999**, *51* (3), 469−479.
(66) Gupta, N. K.; Kim, E. J.; Baek, S.; Bae, J.; Kim, K. S. Ternary Metal Oxide Nanocomposite for Room Temperature H2S and SO2 Gas Removal in Wet Conditions. *Sci. Rep* **2022**, *12* (1), 15387.
(67) Fang, H.; Zhao, J.; Fang, Y.; Huang, J.; Wang, Y. Selective Oxidation of Hydrogen Sulfide to Sulfur over Activated Carbon-Supported Metal Oxides. *Fuel* **2013**, *108*, 143−148.
(68) Davydov, A. A.; Marshneva, V. I.; Shepotko, M. L. Metal Oxides in Hydrogen Sulfide Oxidation by Oxygen and Sulfur Dioxide: I. The Comparison Study of the Catalytic Activity. Mechanism of the Interactions between H2S and SO2 on Some Oxides. *Appl. Catal., A* **2003**, *244* (1), 93−100.
(69) Chughtai, A. R.; Brooks, M. E.; Smith, D. M. Effect of Metal Oxides and Black Carbon (Soot) on SO2/O2/H2O Reaction Systems. *Aerosol Sci. Technol.* **1993**, *19* (2), 121−132.
(70) Yang, Q.; Liu, G.; Falandysz, J.; Yang, L.; Zhao, C.; Chen, C.; Sun, Y.; Zheng, M.; Jiang, G. Atmospheric Emissions of Particulate Matter-Bound Heavy Metals from Industrial Sources. *Sci. Total Environ.* **2024**, *947*, 174467.

https://doi.org/10.1021/acs.est.5c14137
Environ. Sci. Technol. XXXX, XXX, XXX−XXX

(71) Wang, H.; Shadman, F. Effect of Particle Size on the Adsorption and Desorption Properties of Oxide Nanoparticles. *AIChE J.* **2013**, *59* (5), 1502−1510.
(72) Yudanov, I. V.; Genest, A.; Schauermann, S.; Freund, H.-J.; Rösch, N. Size Dependence of the Adsorption Energy of CO on Metal Nanoparticles: A DFT Search for the Minimum Value. *Nano Lett.* **2012**, *12* (4), 2134−2139.
(73) Stará, I.; Matolín, V. The Influence of Particle Size on CO Adsorption on Pd/Alumina Model Catalysts. *Surf. Sci.* **1994**, *313* (1), 99−106.
(74) Linton, R. W.; Loh, A.; Natusch, D. F. S.; Evans, C. A.; Williams, P. Surface Predominance of Trace Elements in Airborne Particles. *Science* **1976**, *191* (4229), 852−854.
(75) Li, Y.; Yang, C.; Fan, H.; Wang, Y.; Duan, M.; Feng, Y.; Lin, J. Enhanced Sulfur Selectivity for H2S Catalytic Oxidation over Fe2O3@UiO-66 Catalyst. *Sep. Purif. Technol.* **2022**, *289*, 120791.
(76) González, L. T.; Rodríguez, F. E. L.; Sánchez-Domínguez, M.; Leyva-Porras, C.; Silva-Vidaurri, L. G.; Acuna-Askar, K.; Kharisov, B. I.; Villarreal Chiu, J. F.; Alfaro Barbosa, J. M. Chemical and Morphological Characterization of TSP and PM2.5 by SEM-EDS, XPS and XRD Collected in the Metropolitan Area of Monterrey, Mexico. *Atmos. Environ.* **2016**, *143*, 249−260.
(77) Neuman, J. A.; Trainer, M.; Brown, S. S.; Min, K.-E.; Nowak, J. B.; Parrish, D. D.; Peischl, J.; Pollack, I. B.; Roberts, J. M.; Ryerson, T. B.; Veres, P. R. HONO Emission and Production Determined from Airborne Measurements over the Southeast U.S. *J. Geophys. Res.:Atmos.* **2016**, *121* (15), 9237−9250.
(78) Zhou, H.; Liu, Z.; Cheng, M.; Zhou, M.; Liu, R. Influence of Coke Combustion on NOx Emission during Iron Ore Sintering. *Energy Fuels* **2015**, *29* (2), 974−984.
(79) Hu, Y.; Naito, S.; Kobayashi, N.; Hasatani, M. CO2, NOx and SO2 Emissions from the Combustion of Coal with High Oxygen Concentration Gases. *Fuel* **2000**, *79* (15), 1925−1932.
(80) Ma, P.; Quan, J.; Dou, Y.; Pan, Y.; Liao, Z.; Cheng, Z.; Jia, X.; Wang, Q.; Zhan, J.; Ma, W.; Zheng, F.; Wang, Y.; Zhang, Y.; Hua, C.; Yan, C.; Kulmala, M.; Liu, Y.; Huang, X.; Yuan, B.; Brown, S. S.; Liu, Y. Regime-Dependence of Nocturnal Nitrate Formation via N2O5 Hydrolysis and Its Implication for Mitigating Nitrate Pollution. *Geophys. Res. Lett.* **2023**, *50* (24), No. e2023GL106183.
(81) Kong, L. D.; Zhao, X.; Sun, Z. Y.; Yang, Y. W.; Fu, H. B.; Zhang, S. C.; Cheng, T. T.; Yang, X.; Wang, L.; Chen, J. M. The Effects of Nitrate on the Heterogeneous Uptake of Sulfur Dioxide on Hematite. *Atmos. Chem. Phys.* **2014**, *14* (17), 9451−9467.

https://doi.org/10.1021/acs.est.5c14137
Environ. Sci. Technol. XXXX, XXX, XXX−XXX